Lock-exchange experiments with an autocatalytic reaction front

I. Bou Malham,[1] N. Jarrige,[1] J. Martin,[1] N. Rakotomalala,[1] L. Talon,[1] and D. Salin[1,2,a)]
[1]*University Pierre et Marie Curie, University Paris-Sud, CNRS. Lab FAST, Bat. 502, Campus Universitaire, Orsay, F-91405, France*
[2]*Institut Universitaire de France, 103 Bd Saint Michel, 75005 Paris, France*

(Received 20 July 2010; accepted 11 October 2010; published online 28 December 2010)

A viscous lock-exchange gravity current corresponds to the reciprocal exchange of two fluids of different densities in a horizontal channel. The resulting front between the two fluids spreads as the square root of time, with a diffusion coefficient reflecting the buoyancy, viscosity, and geometrical configuration of the current. On the other hand, an autocatalytic reaction front between a reactant and a product may propagate as a solitary wave, namely, at a constant velocity and with a stationary concentration profile, resulting from the balance between molecular diffusion and chemical reaction. In most systems, the fluid left behind the front has a different density leading to a lock-exchange configuration. We revisit, with a chemical reaction, the classical situation of lock-exchange. We present an experimental analysis of buoyancy effects on the shape and the velocity of the iodate arsenous acid autocatalytic reaction fronts, propagating in horizontal rectangular channels and for a wide range of aspect ratios (1/3 to 20) and cylindrical tubes. We do observe stationary-shaped fronts, spanning the height of the cell and propagating along the cell axis. Our data support the contention that the front velocity and its extension are linked to each other and that their variations scale with a single variable involving the diffusion coefficient of the lock-exchange in the absence of chemical reaction. This analysis is supported by results obtained with lattice Bathnagar-Gross-Krook (BGK) simulations Jarrige *et al.* [Phys. Rev. E **81**, 06631 (2010)], in other geometries (like in 2D simulations by Rongy *et al.* [J. Chem. Phys. **127**, 114710 (2007)] and experiments in cylindrical tubes by Pojman *et al.* [J. Phys. Chem. **95**, 1299 (1991)]), and for another chemical reaction Schuszter *et al.* [Phys. Rev. E **79**, 016216 (2009)]. © *2010 American Institute of Physics*. [doi:10.1063/1.3507899]

I. INTRODUCTION

We address the issue of the gravity current produced by a chemically induced lock-exchange. In a lock-exchange experiment, fluids with different densities, initially at rest in a vessel, are separated by a vertical barrier (the lock gate). When the gate is withdrawn, differences in buoyancy cause the denser fluid to flow in one direction along the bottom of the vessel, while the lighter one flows in the opposite direction at the top of the vessel.[5–9] The spreading rate of the current depends on two parameters, namely, the relative height of the release (i.e., the denser fluid) and the density ratio between the light and the heavy fluids. When the density difference between the two fluids is small, the currents are known as Boussinesq currents. In the present paper, we address the issue of the lock-exchange generated by an autocatalytic chemical reaction. Autocatalytic reaction fronts between a reactant and a product may propagate as solitary waves, namely, at a constant velocity and with a stationary concentration profile, resulting from a balance between molecular diffusion and chemical reaction.[10–14] In the presence of a forced hydrodynamic flow field, such reaction fronts still propagate as solitary waves but with an enhanced propagation velocity and with a front shape reminiscent of a flame front.[15,16] In most systems, the fluid left behind the reaction front has a different density, which may induce gravitational instabilities of horizontal fronts[14,17] or buoyancy driven flows for tilted fronts. We note, however, that the density contrast is usually tiny (less than 0.1%) and that typical resulting velocities are of the order of 10–100 μm/s. Therefore, the lock-exchange with chemical reaction corresponds to Boussinesq viscous lock-exchange.[5,7–9] In the absence of chemistry the lock-exchange issue is well documented: it results in a front spreading as the square root of time, with a diffusion coefficient reflecting the buoyancy, viscosity, and geometrical configuration of the current. It has been computed for a porous medium,[5] a 2D Stokes flow[8,18] between two parallel horizontal boundaries separated by a vertical height, H, a tube[7] and recently for rectangular channels of horizontal thickness, b, and vertical height, H.[9] In the presence of chemistry, pioneering experiments in cylindrical tubes have been performed with the iodate arsenous acid (IAA) autocatalytic reaction.[3] More recently, numerical simulations by Rongy *et al.*[2] addressed the issue of buoyancy driven 2D Stokes flow between two parallel boundaries separated by a vertical height, H, for the IAA reaction. Recent experiments by Schuszter *et al.*[4] investigated the H dependence of the front extension for the chlorite-tetrathionnate (CT) autocatalytic reaction propagating in a rectangular cell of large aspect ratio, $\Gamma = H/b$. Also for large aspect ratios, Jarrige *et al.*[1] performed 2D numerical simulations to modelize the 3D IAA autocatalytic reaction propagating in a rectangular cell.

We present an experimental analysis of buoyancy effects on the shape and the velocity of the IAA autocatalytic

a)Electronic mail: dominique.salin@upmc.fr.

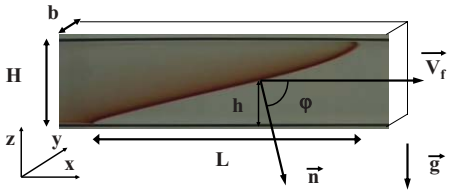

FIG. 1. Picture of the stationary IAA autocatalytic reaction front in a rectangular cell of height $H = 15$ mm and thickness $b = 1$ mm. $\vec{V}_f$ is the velocity of the front, propagating from left to right. $\vec{n}$ is the local unit vector normal to the interface, $z = h(x)$, and $\varphi = (\vec{n}, \vec{x})$ is the angle between $\vec{n}$ and the horizontal cell axis, x. $\vec{g}$ is the gravity acceleration. L is the extension length of the front.

reaction fronts, propagating in a horizontal rectangular channel of dimensions $H \times b$ over a wide range of aspect ratios ($\Gamma = 1/3$ to 20) and in cylindrical tubes. We observe stationary-shaped fronts, spanning the height of the cell and propagating along the horizontal cell axis. We analyze the scaling law for the shape and the velocity of the fronts and we develop a model which accounts for them in our rectangular cells and tubes. Moreover, it also accounts for previous experiments in cylindrical tubes by Pojman *et al.*,[3] for 2D numerical simulations by Jarrige *et al.*[1] and Rongy *et al.*[2] and for experiments with a different chemistry by Schuszter *et al.*[4]

II. EXPERIMENTS

We analyze in the present work the reaction front in rectangular cells (Fig. 1). We performed experiments with the IAA autocatalytic reaction:

$$3H_3AsO_3 + IO_3^- + 5I^- \longrightarrow 3H_3AsO_4 + 6I^-. \quad (1)$$

The reaction is autocatalytic in iodide (I^-). The concentrations used are: $[IO_3^-]_0 = 7.5$ mM, $[H_3AsO_3]_0 = 25$ mM. With such a ratio, $[H_3AsO_3]_0/[IO_3^-]_0 > 3$, the arsenous is in excess[13] and the front can be localized by the transient iodine generated during the reaction. The diffusion-reaction equation governing the third-order autocatalytic IAA reaction[13] reads:

$$\frac{\partial C}{\partial t} = D_m \triangle C + \frac{1}{\tau} C^2 (1 - C), \quad (2)$$

where C is the concentration of the autocatalytic reactant (iodide), normalized by the initial concentration of iodate ($C = [I^-]/[IO_3^-]_0$), D_m is the molecular diffusion coefficient, and τ is the reaction time. The balance between diffusion and reaction leads to a solitary wave of constant velocity V_χ and width l_χ,[12–14] which are given by

$$V_\chi = \sqrt{\frac{D_m}{2\tau}}, \quad l_\chi = D_m / V_\chi. \quad (3)$$

Physically, the propagation velocity of the reaction is controlled by the combined effects of the chemical reaction rate $1/\tau$, and the diffusion of the catalyzing burnt product into the fresh solution, as $C > 0$ is a necessary condition for the reaction to begin. The above expression of V_χ reflects such combined effects. Along the same line, the diffusive spreading of the front is mitigated by the chemical reaction, which turns the diffusing low concentration $C \simeq 0$ into $C \simeq 1$, in a characteristic time τ. This is in accordance with the expression for l_χ [Eq. (3)], which scales as the diffusion length during the time τ, namely, $l_\chi \simeq \sqrt{D_m \tau}$. Instead of the classical starch, used to detect the transient iodine, we use, as Ref. 19, polyvinyl alcohol (PVA) at a concentration of 6 kg/m^3 which is much more sensitive and gives also a good optical contrast (Figs. 1 and 2). We also note that the PVA, which forms a complex with iodine, lowers the molecular diffusion of species.[20] With the above concentrations, one can predict[12,21] a typical front velocity $V_\chi \simeq 100\,\mu$m/s, whereas in the presence of PVA, we measure $V_\chi \simeq 10\,\mu$m/s, which is 1 order of magnitude smaller.

For IAA, thermal effects are negligible[3,22] and the buoyancy difference is mainly solutal. The measured density difference is $\Delta\rho = \rho^+ - \rho^- = (0.23 \pm 0.03)$ kg/m^3, where ρ^+ and ρ^- correspond to the fresh and burnt solutions, respectively. The viscosity is not changed by the reaction, and is equal to $\eta = (1.15 \pm 0.05)$ mPa s. Note that, although the measurement of the viscosity is accurate, the lack of temperature control leads to an uncertainty of 10% on the viscosity. We tested the viscosity effect on the front propagation, by adding natrosol, in order to increase the viscosity of the solution up to a factor 35. Surprisingly, such a viscosity increase did not affect the chemical velocity V_χ in the range of parameters used: as D_m is inversely proportional to the viscosity,[23] this would mean that both D_m and τ vary by the same relative amount [after Eq. (3)].

We used borosilicate rectangular cells of height H, thickness b, and typical length 30 cm (Fig. 1). The cell thickness was varied from 200 μm to 14 mm and its width from 4 mm to 20 mm. With such values, we cover a wide range of aspect ratios, $\Gamma = H/b = 1/3$, 0.4, 1, 3, 6, 10, 15, 20. Note that large aspect ratios correspond to the so-called Hele-Shaw cells (two infinite parallel plates separated by a small gap of width b). Some experiments have been also performed in horizontal cylindrical tubes of diameters $d = 4.65$ and 6.93 mm, in order to extend the range of diameters used by Pojman *et al.*[3]

Initially, the cell is full of fresh reactant and is held vertical, with its section $H \times b$ in the horizontal plane. The reaction is initiated with a small amount of product at the top boundary of the cell, which is then sealed. The downward chemical wave velocity is measured in this stable configuration. We obtained typically $V_\chi = (11 \pm 2)\,\mu$m/s, which corresponds to a chemical front width $l_\chi = D_m/V_\chi \simeq 100\,\mu$m with $D_m \simeq 10^{-9}$ m^2/s. After a while, the cell is rotated by an angle of 90°, with its section $H \times b$ in the vertical plane (Fig. 1) and the front is recorded with a video camera. In all instances, the so-obtained fronts evolve toward stationary-shaped fronts, traveling at a constant velocity V_f. The front velocity V_f is then measured and the stationary shape is characterized. Figures 1 and 2 display pictures of typical fronts, traveling from left to right. Whatever the cell size and the aspect ratio, the front shape looks the same: from the bottom to the top of the cell, the front is almost linear (at least in the half bottom part of the cell) and starts to curve near the top boundary. To characterize this front shape, Jarrige *et al.*[1] tried different measurements such as the tilt angle with respect to the cell axis (the average angle or its value at midheight) or the extension length of the front. None of those measurements was better than the others in terms of data analysis. Moreover, as we will see later on, the so-obtained information are somehow

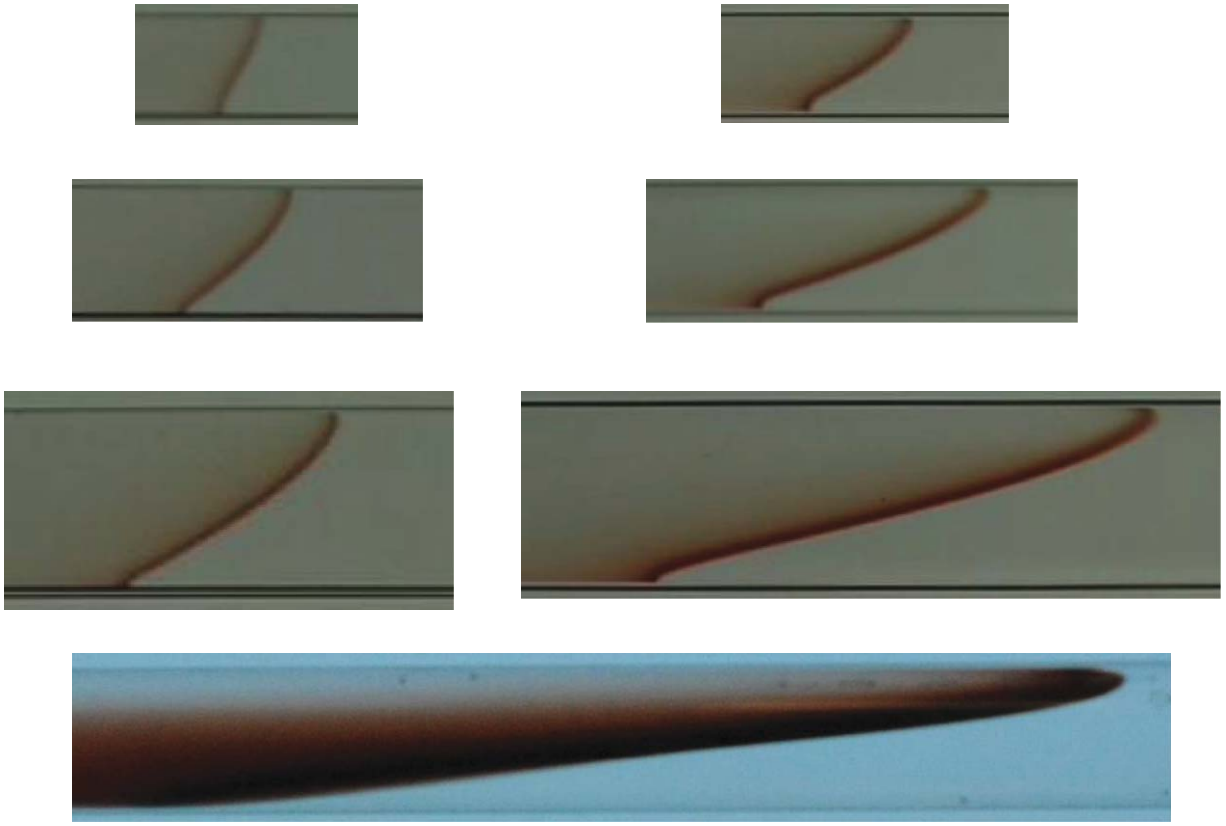

FIG. 2. Pictures of the stationary IAA autocatalytic reaction fronts in six rectangular cells and in a cylindrical tube of diameter 6.93 mm (bottom). From top to bottom, first row: $H = 4$ mm, $b = 0.2$ mm (left), and $b = 0.4$ mm (right). Second row: $H = 6$ mm, $b = 0.3$ mm (left), and $b = 0.6$ mm (right). Third row: $H = 8$ mm, $b = 0.4$ mm (left), and $b = 0.8$ mm (right).

redundant with the front velocity V_f. Therefore, to characterize the front shape, we chose arbitrary the front extension, L, as defined by Jarrige *et al.*[1] and displayed in Fig. 1: L is the distance over which the cross-section averaged concentration varies from 1% to 99%. Note that the latter quantity is very close to the length used by Rongy *et al.*[2] We observed that L increases with the height H, at fixed thickness b, and with b at fixed H. These tendencies, evidenced by Fig. 2, were also observed in our other experiments not shown here. The values of the front velocities and extensions range typically from 20 μm/s to 100 μm/s and 1 mm to 20 cm, respectively, which correspond to rather large front extensions.

III. RESULTS: FRONT VELOCITY AND EXTENSION

In this paper, we will focus mainly on the measurements of the velocity V_f and of the extension L of the front. Since the Reynolds number is small, $Re = \rho V_f b/\eta \ll 1$, the fluid flow is in the viscous regime. A viscous buoyant characteristic velocity V_g may thus be defined as:

$$V_g = \frac{b^2 \Delta\rho g}{12\eta}. \tag{4}$$

This is also the Darcy velocity, used by Huppert and Woods,[5] which corresponds to the balance between the buoyancy and the viscous drag forces in a porous medium of permeability $\kappa = b^2/12$. Moreover, since all the length scales b, H, and L are much larger than the chemical length, $l_\chi \simeq 100\,\mu$m (i.e., the front thickness), the propagation of the chemical front is in the so-called eikonal regime.[15] In such conditions, as it was shown by Jarrige *et al.*[1] the front velocity, V_f, and its extension, L, depend only on two nondimensional parameters:

$$\Gamma = H/b, \qquad \epsilon = V_g/V_\chi, \tag{5}$$

where Γ is the aspect ratio of the cell and ϵ is the ratio of the Darcy velocity to the chemical velocity. This is evidenced by our experiments: at a fixed aspect ratio Γ, if the cell thickness b and the fluid viscosity are increased by a factor 2 and 4, respectively, keeping thus V_g (and ϵ) constant, the front velocity and shape are unchanged. We note however that if the front propagation were not in the eikonal regime, another nondimensional number would be necessary (such as H/l_χ).

Figure 3 displays a log–log plot of the reduced front velocity, V_f/V_χ, and of the reduced front extension, L/H, versus the buoyant velocity ϵ, for rectangular cells of different aspect ratios, Γ, for cylindrical tubes (in this case, the tube diameter d replaces the cell thickness b), and for the lattice BGK numerical simulations by Jarrige *et al.*[1] Note that we obtain variations of V_f/V_χ and L/H over one decade whereas ϵ varies over more than two decades. In both figures, the data, for each value of Γ, are somehow dispersed. This is related to the accuracy of our measurements: the uncertainty on ϵ is of the order of 50% (15% on $\Delta\rho$, 10% on the viscosity, and 20% on V_χ) and that on V_f/V_χ is about 20%. Note also that the

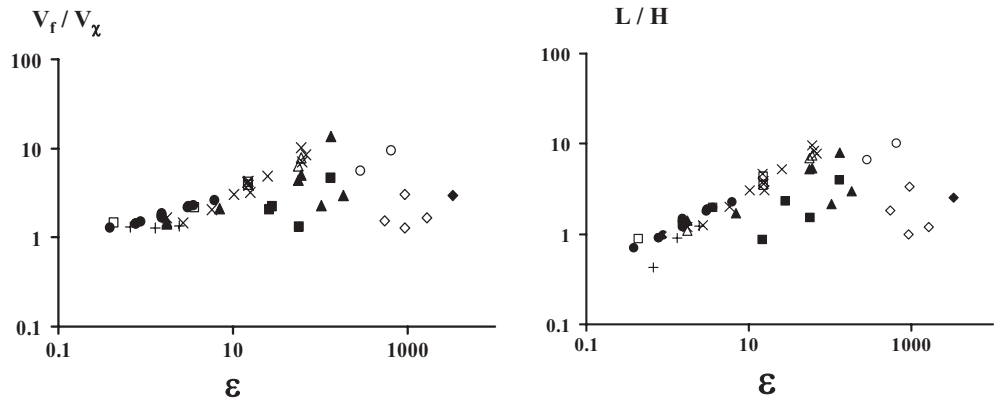

FIG. 3. Log–log plot of the nondimensional front velocity, V_f/V_χ (left), and of the nondimensional front extension, L/H (right), versus the buoyancy characteristic velocity, $\epsilon = V_g/V_\chi$, for different aspect ratios: $\Gamma = 1/3$ (◇) and 0.4 (♦), 1 (■), 3 (▲), 6 (△), 10 (×), 15 (□), and 20 (+). The open circles (○) correspond to cylindrical tubes where the tube diameter, d, replaces the cell thickness, b, in the expressions of ϵ and Γ. The bullets (●) correspond to the lattice BGK numerical simulations of Jarrige *et al.* (Ref. 1) performed at $\Gamma = 10$. The overall accuracies in ϵ and V_f/V_χ are of the order of 50% and 20%, respectively.

same value of Γ may correspond to cells of different sizes, H and b. Although mitigated by the dispersion of the data, some trends may however be noticed in Fig. 3. First, for a given Γ, increasing ϵ leads to larger front extensions and higher front velocities. This result is expected since ϵ estimates the relative strength of buoyancy. In addition, the two figures display a very similar trend, suggesting that the velocity of the front and its extension are likely to be linked, similarly as it was observed and understood in the forced advection of chemical fronts by Edwards[15] and Leconte *et al.*[16] Such a link is evidenced, in our present case, by Fig. 4, which displays the ratio V_f/V_χ versus the ratio L/H. All the different data merge fairly well, which shows that the dispersion of the data of Fig. 3 is mostly due to the lack of accuracy in the estimation of ϵ. Moreover, the data compare well with a prediction by Jarrige *et al.*,[1] in the framework of the eikonal regime. In this regime, the front is very thin and the following advection–diffusion–reaction equation for the concentration C (Ref. 15)

$$\frac{\partial C}{\partial t} + \vec{U}\cdot\vec{\nabla}C = D_m\triangle C + \frac{1}{\tau}C^2(1-C) \tag{6}$$

(where $\vec{U}$ is the hydrodynamic fluid velocity) can be replaced by its eikonal counterpart, which applies at the front surface. Therefore,

$$\vec{V}_f\cdot\vec{n} = \vec{U}\cdot\vec{n} + V_\chi, \tag{7}$$

where $\vec{n} = (\cos\varphi, 0, -\sin\varphi)$ is the local unit vector normal to the interface (Fig. 1), $\varphi = (\vec{n}, \vec{x})$ is the angle between $\vec{n}$ and the horizontal axis, x, of the cell, and $\vec{U}$ is the fluid velocity at the front.

In 2D simulations, the normal component of the fluid velocity was found to be zero at one point of the front, a little above the middle of the cell.[1,2] There, Eq. (7) writes $V_\chi \simeq V_f\cos\varphi$. Moreover, an estimation of φ may be obtained by approximating roughly the 2D front by a straight line (or a planar surface, in our 3D experiments). We obtain $\tan\varphi \simeq L/H$, and thus

$$\frac{V_f}{V_\chi} = \sqrt{1+\left(\frac{L}{H}\right)^2}. \tag{8}$$

This expression is the line through the data in Fig. 4. It is worth noting that for large extensions, we have roughly $V_f/V_\chi \simeq L/H$. Such a proportionality between the front velocity and its extension was also obtained in the 2D simulations by Rongy *et al.*[2] The latter simulations, displayed as a dashed straight line in Fig. 4, correspond indeed to rather large extensions, as will be discussed below. We also put the numerical data of Jarrige *et al.*[1] which correspond to smaller extensions and are therefore more sensitive to the exact form of Eq. (8). In conclusion, our experiments and lattice BGK numerical simulations,[1] as well as the simulations in a 2D geometry[2] support the above relationship [Eq. (8)].

We have shown that a simple relationship holds between our two measured quantities. In Sec. IV, we will show that a second relationship can be deduced from the lock-exchange gravity current diffusive behavior without chemistry. With

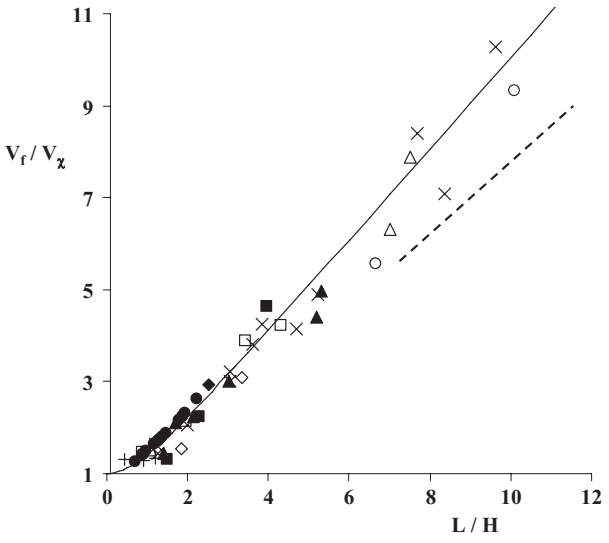

FIG. 4. Nondimensional front velocity, V_f/V_χ, versus the nondimensional front extension, L/H. The symbols are the same as in Fig. 3. The dashed straight line of slope 0.74 corresponds to the 2D simulations of Rongy *et al.* (Ref. 2) The solid line through the data corresponds to the relationship found from the eikonal regime [Eq. (8)] in Jarrige *et al.* (Ref. 1) which, for large extensions, leads to $V_f/V_\chi \simeq L/H$.

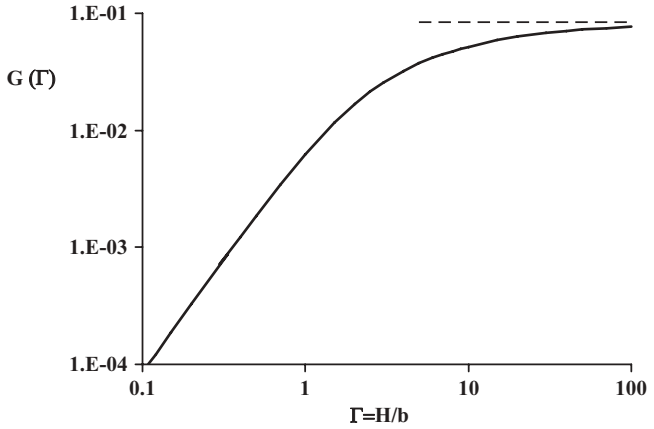

FIG. 5. Normalized lock-exchange diffusion coefficient for rectangular cells of aspect ratio $\Gamma = H/b$ [from Martin *et al.* (Ref. 9)]. The coefficient is normalized by $b^2 H \Delta\rho\, g/\eta$ leading to the function $G(\Gamma)$ [Eq. (9)]. With such a normalization, the dashed horizontal line of value 1/12 corresponds to a Hele–Shaw cell of infinite aspect ratio, i.e., a homogeneous porous medium.

these two relationships in hand, we will then propose a prediction for the propagation of a buoyant reaction front as a function of our control parameters.

IV. RELATION BETWEEN CHEMICAL REACTION AND PURE LOCK-EXCHANGE

In the absence of chemistry, a viscous lock-exchange gravity current leads to the spreading of the fluid interface that grows as the square root of time.[5,7–9,18] The corresponding effective diffusion coefficient D_{lock} depends on buoyancy, viscosity, and on the geometry of the cell. For a rectangular cell, its expression, derived very recently by Martin *et al.*,[9] involves a function of the aspect ratio, $G(\Gamma)$, such that

$$D_{\text{lock}} = b^2 H \frac{\Delta\rho\, g}{\eta} G(\Gamma). \tag{9}$$

The function $G(\Gamma)$ is plotted in Fig. 5 and displays a plateau of value 1/12 at large aspect ratios, which corresponds to the Hele–Shaw cell limit ($b \ll H$), or equivalently, to a 2D porous medium. We have seen in Sec. II that the interplay between an autocatalytic reaction, which sharpens the chemical front, and the molecular diffusive mixing, which tends to spread the front, results in a stationary front of thickness l_χ and velocity V_χ such that $l_\chi\, V_\chi = D_m$ [Eq. (3)]. In the presence of gravity, an analogous behavior involving the effective diffusion coefficient D_{lock} would lead to $V_f\, L = D_{\text{lock}}$. Such a conjecture is addressed in Fig. 6, which displays a log–log plot of the product $V_f\, L$ as a function of D_{lock} for different aspect ratios ranging from small values ($\Gamma = 1/3$) to large ones ($\Gamma = 20$). Note that for the two data points corresponding to cylindrical tubes (open circles in Fig. 6), we used the lock-exchange diffusion coefficient in a tube defined in Sec. VI. All the data reasonably collapse onto a straight line

$$V_f\, L = a\, D_{\text{lock}}, \tag{10}$$

where the factor a can be evaluated with a linear fit to our data, yielding $a = (1.8 \pm 0.1)$. Combining this second

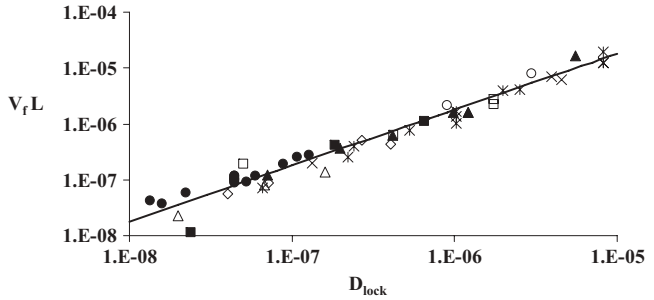

FIG. 6. Product of the front velocity by the length of the front, $V_f\, L$, versus the lock-exchange diffusion coefficient, D_{lock}, for various cell aspect ratios, Γ. Same symbols as in Fig. 3. The full line corresponds to Eq. (10).

empirical relationship [Eq. (10)] between the two measured quantities V_f and L with Eq. (8) leads to

$$\left(\frac{V_f}{V_\chi}\right)^2 = (\sqrt{1 + 4\,a^2\,\Lambda^2} + 1)/2 \tag{11}$$

and

$$\left(\frac{L}{H}\right)^2 = (\sqrt{1 + 4\,a^2\,\Lambda^2} - 1)/2, \tag{12}$$

where V_f/V_χ and L/H express themselves as functions of one single variable,

$$\Lambda = \frac{D_{\text{lock}}}{H\,V_\chi}. \tag{13}$$

This result is evidenced by Fig. 7, which displays $(V_f/V_\chi)^2$ and $(L/H)^2$ as functions of Λ: all the experimental and numerical data shown in Fig. 3 collapse onto the two curves given by Eqs. (11) and (12), and using $a = 1.8$. We note that the latter expressions still fairly hold, within the experimental error, for $L/H \simeq 1$ and $V_f/V_\chi \simeq 1$, which is even beyond expectations, as we recall that the expressions of D_{lock} were

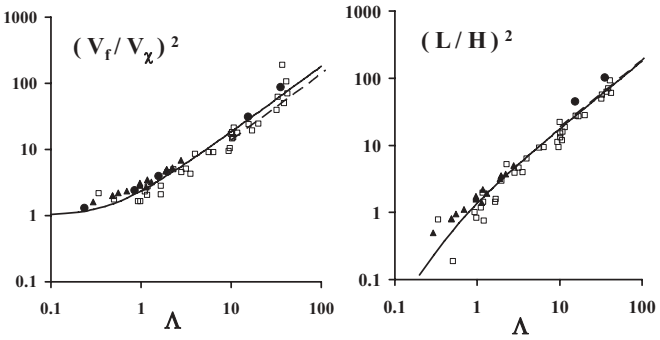

FIG. 7. Log–log plot of $(V_f/V_\chi)^2$ (left) and $(L/H)^2$ (right) versus the scaling variable Λ, where $\Lambda = D_{\text{lock}}/(H\,V_\chi)$ for rectangular cells and $\Lambda = D_{\text{tube}}/(d\,V_\chi)$ for cylindrical tubes. The symbol (□) corresponds to the experiments plotted in the previous figures with different symbols. The symbol (▲) corresponds to lattice BGK simulations of Jarrige *et al.* (Ref. 1) for small aspect ratios whereas the dashed line represents the 2D numerical simulations of Rongy *et al.* (Ref. 2) between two parallel boundaries separated by a height, H. The full line on the graphs corresponds to our empirical law [Eqs. (11) and (12)]. Note that the dashed line on the right figure is hardly distinguishable from the full line for $\Lambda > 10$. The circles (●) correspond to cylindrical tube experiments: the two large Λ values ($\Lambda > 10$) correspond to our experiments and the three data points at low values ($\Lambda < 10$) on the left figure correspond to the data of Pojman *et al.* (Ref. 3).

obtained by the different authors,[5,7–9,18] using the assumption $L/H > 1$ (and thus, $V_f > V_\chi$). We also note that in the latter range, Eqs. (11) and (12) simplify into

$$\frac{V_f}{V_\chi} = \frac{L}{H} \simeq 1.35\sqrt{\Lambda}. \tag{14}$$

This power law relationship is indeed a good approximation for $\Lambda > 1$. We notice that the parameter, Λ, which controls the interplay between the propagation of a chemical front and the induced gravity lock-exchange, is the ratio of two velocities:

$$\Lambda = \frac{V_{\text{lock}}}{V_\chi}, \quad \text{where} \quad V_{\text{lock}} = \frac{D_{\text{lock}}}{H} = 12\, V_g\, G(\Gamma). \tag{15}$$

Similarly to V_g [defined in Eq. (4)], V_{lock} estimates the magnitude of the velocity that may be induced by buoyancy. However, it is more relevant as it accounts for the aspect ratio of the cell of interest [through $G(\Gamma)$]. Note also that for infinitely thin Hele-Shaw cells ($\Gamma \to \infty$), $V_{\text{lock}} = V_g$.

V. FRONT REACTION PROFILE

Our prediction for the front velocity should enable to compute the front shape using the eikonal equation [Eq. (7)], which can be rewritten, at each vertical location, $z = h(x)$, of the interface, as:

$$V_f \cos\varphi = u(h)\cos\varphi - w(h)\sin\varphi + V_\chi, \tag{16}$$

where $u(h)$ and $w(h)$ are, respectively, the horizontal and vertical components of the gap-averaged velocity field at the front. Using $\partial h/\partial x = \cos\varphi/\sin\varphi$ allows to write Eq. (16) in the form:

$$V_f \frac{\partial h}{\partial x} = u \frac{\partial h}{\partial x} - w + V_\chi \sqrt{1 + \left(\frac{\partial h}{\partial x}\right)^2}. \tag{17}$$

The horizontal flux of reactant, q, at the location x is defined by

$$q = \int_0^h u(x,z)dz, \tag{18}$$

the derivative of which writes

$$\begin{aligned}\frac{\partial q}{\partial x} &= u\frac{\partial h}{\partial x} + \int_0^h \frac{\partial u}{\partial x}dz \\ &= u\frac{\partial h}{\partial x} - \int_0^h \frac{\partial w}{\partial z}dz = u\frac{\partial h}{\partial x} - w(h),\end{aligned} \tag{19}$$

where the incompressibility equation, $\partial u/\partial x + \partial w/\partial z = 0$, has been used. From Eqs. (17) and (19) we obtain

$$V_f \frac{\partial h}{\partial x} = \frac{\partial q}{\partial x} + V_\chi \sqrt{1 + \left(\frac{\partial h}{\partial x}\right)^2}. \tag{20}$$

We note that Eq. (20) is simply the reactant mass conservation

$$\frac{\partial h}{\partial t} + \frac{\partial q}{\partial x} + V_\chi \sqrt{1 + \left(\frac{\partial h}{\partial x}\right)^2} = 0$$

for a front propagating at constant velocity, $\partial h/\partial t = -V_f(\partial h/\partial x)$, and with a particular source term for the chemistry under the eikonal condition.

The new Eq. (20) for the shape of the front requires, however, to compute first the flux q, using Eq. (18), if the expression of the horizontal velocity $u(x,z)$ is available. Unfortunately, the latter writes generally as $u(x,z) = u(z, h(x), \partial h/\partial x, \ldots)$ and contains complicated x dependence. However, an expression for rectangular cells has been obtained by Martin *et al.*,[9] using a parallel flow approximation, which leads to a flux of the form:

$$q = -\frac{b^2 H\, \Delta\rho\, g}{12\eta}\, f_\Gamma(h/H)\, \frac{\partial h}{\partial x}, \tag{21}$$

where the function $f_\Gamma(h/H)$ has been calculated by Martin *et al.*[9]

For a known front velocity V_f [Eq. (11)], the integration of Eq. (20) provides the front profile. A typical profile, so obtained using MATHEMATICA software, is compared to the corresponding experimental one in Fig. 8. The shapes are almost the same, but we note however that the numerical extension is slightly smaller than the experimental one. This discrepancy might be due to the condition of a small slope of the interface (i.e., $\partial h/\partial x \ll 1$), required for the parallel flow approximation to apply. Obviously, this condition is not fulfilled in the vicinity of the upper boundary.

VI. COMPARISON AND ANALYSIS OF RELATED PAPERS

In this section, we compare our empirical law with results previously obtained for similar configurations. In their pioneering experiments, Pojman *et al.*[3] used cylindrical tubes of diameter $d = 0.94$, 1.78, and 2.4 mm to study the propagation of an IAA autocatalytic reaction and the so-called convection pattern. These experiments have been modeled, using a 2D calculation by Vasquez *et al.*[24] In Pojman *et al.*,[3] the velocities V_χ and V_f were measured in vertical and horizontal tubes, respectively. The so-obtained values of $(V_f/V_\chi)^2$ are plotted in Fig. 7 (full circles), as functions of the corresponding variable $\Lambda = D_{\text{tube}}/(dV_\chi)$, where d is the tube diameter and D_{tube} is the lock-exchange coefficient in a tube, computed by Hinch[18] and Séon *et al.*[7]

$$D_{\text{tube}} = 0.0054\, \frac{d^3 \Delta\rho\, g}{\eta}. \tag{22}$$

Note that we have extended the range of Λ explored by Pojman *et al.*,[3] with experiments in cylindrical tubes of diameters 4.65 and 6.93 mm, which provide values of both V_f/V_χ and L/d for larger values of Λ. All these data displayed in Fig. 7 compare very well with the extension of our empirical model to the tube geometry using $\Lambda = D_{\text{tube}}/(dV_\chi)$ and L/d.

Another geometry was recently addressed by Rongy *et al.*[2] with 2D numerical simulations of "Buoyancy-driven convection around chemical fronts traveling in covered horizontal solution layers." In this work, the authors investigated the reaction front between two infinite parallel horizontal boundaries distant of H. For a fixed value $H/l_\chi \simeq 7$, they found that the velocity and the extension of the resulting stationary propagating fronts obeyed the relations:

$$V_f \simeq 1.12\, V_\chi \sqrt{\text{Ra}}, \tag{23}$$

$$L \simeq 10.6\, l_\chi \sqrt{\text{Ra}}, \tag{24}$$

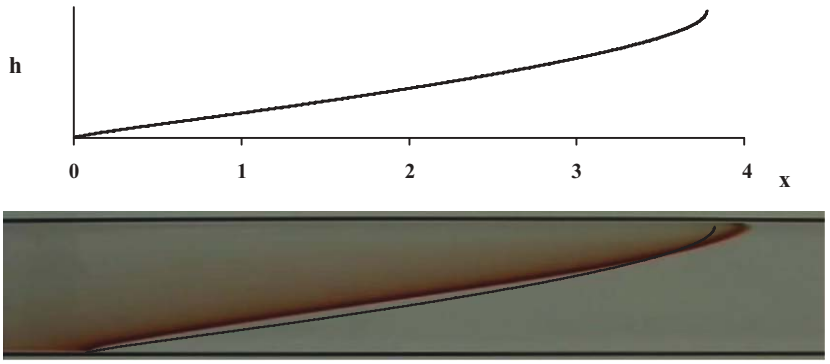

FIG. 8. Top: pseudointerface, $z = h(x)$, between the reactant and the product obtained by integration of Eq. (20), using the front velocity, V_f, measured in the experiment. Bottom: a tentative superimposition of the calculated front and the experimental front.

where the Rayleigh number is defined as:

$$\mathrm{Ra} = \frac{\Delta\rho\, g\, l_\chi^3}{2^{3/2}\,\eta\, D_m}$$

First, their results lead to

$$V_f/V_\chi \simeq 0.74 L/H. \tag{25}$$

This relationship, obtained in the range $L/H \simeq 10$, is depicted as a dashed straight line in Fig. 4. It gives a lower bond, very close to our data. We note that it is also similar, although 25% lower, to the behavior of our relationship [Eq. (8)], which writes, for $L/H \gg 1$, $V_f/V_\chi \simeq L/H$. We recall however that the latter expression was obtained assuming an eikonal regime ($H/l_\chi \gg 1$). As the eikonal regime conditions were marginally fulfilled ($H/l_\chi \simeq 7$) in the simulations of Rongy *et al.*,[2] a different coefficient is not unexpected. Moreover, in the 2D geometry addressed by Rongy *et al.*,[2] the nonreacting lock-exchange gravity currents are known to spread also as the square root of time[8,9,18] with an effective diffusion coefficient:

$$D_{\mathrm{lock2D}} = 0.0085\, H^3\, \frac{\Delta\rho\, g}{\eta}. \tag{26}$$

This defines the corresponding variable $\Lambda = D_{\mathrm{lock2D}}/HV_\chi$, which can be used to rewrite the expressions of V_f/V_χ and L/H obtained by Rongy *et al.*[2] as

$$\frac{V_f}{V_\chi} \simeq 1.0\sqrt{\Lambda}, \tag{27}$$

$$\frac{L}{H} \simeq 1.4\sqrt{\Lambda}. \tag{28}$$

The above expressions, plotted in Fig. 7, are very close to our case of interest, despite the difference of regime. Note in particular that the so-obtained expression for L/H differs by less than 5% from our Eq. (14), $L/H \simeq 1.35\sqrt{\Lambda}$. Note also that our model accounts for the scalings, $L \propto H^2$ and $V_f \propto H$, observed by Rongy *et al.*[2]

More generally, our empirical model may be useful to provide scaling laws in an understandable way, as it can easily be extended to different experimental conditions. It may be applied, for example, to the case of a different kinetics, as the one of the CT autocatalytic reaction, which leaves a heavier fluid behind the front. This reaction was recently used by Schuszter *et al.*[4] to study reacting gravity currents in horizontal rectangular cells. Schuszter *et al.*[4] measured the effects of the cell aspect ratio, Γ (from $\Gamma = 10$ to $\Gamma = 40$, and for a fixed cell thickness $b = 1$ mm) and of the chemical composition, $[S_4O_6^{2-}]$ (ranging between 3.75 and 6.25 mM), on the front extension, L, called mixing length in their work. They found that L did not depend on $[S_4O_6^{2-}]$ (within the error bars) and was given by

$$L = (2.24 \pm 0.12) H^{1.19\pm0.04}, \tag{29}$$

where H and L are expressed in centimeters. In the reported CT experiments, the eikonal regime conditions are fulfilled ($H/l_\chi > 100$). Accordingly, our model should apply as the kinetics should be accounted through the value of V_χ (which is 10 times faster for CT than for IAA), and the details of the reaction should not come into play. We obtain from Eqs. (9), (13), and (14), $L/H \simeq 1.35\sqrt{\Lambda} \simeq 4.7\sqrt{\epsilon\, G(\Gamma)}$ (where $\epsilon = V_g/V_\chi$). Thus, for a given Γ, our model predicts a growing of the front extension, L, as $\sqrt{\epsilon}$. In the CT reaction, the characteristic velocities were found to scale as $V_\chi \propto [S_4O_6^{2-}]^{3/2}$ (Ref. 25) and $V_g \propto [S_4O_6^{2-}]$ (Ref. 4), yielding $\epsilon \propto [S_4O_6^{2-}]^{-1/2}$. Given the range covered by $[S_4O_6^{2-}]$, the corresponding variations of ϵ are about 20%. Consequently, our model predicts a variation of about 10% of the front extension, L, which lies within the error bar of Eq. (29). As for the power law variation of L with H, we note that in the range $\Gamma \in [10, 40]$ explored by Schuszter *et al.*,[4] the log–log plot of $G(\Gamma)$ displayed in Fig. 5 may be approximated by a straight line of slope 0.24 ± 0.06. Such an approximation would lead to $L \propto H^{1.12\pm0.06}$, which is also in line with Eq. (29).

VII. CONCLUSION

We have measured the effect of an autocatalytic chemical reaction on a viscous lock-exchange horizontal gravity current in rectangular cells, over a wide range of aspect ratios and sizes. We observed stationary-shaped fronts spanning the height of the cell and propagating at constant velocity. A clear relationship between the front extension and its velocity has been determined and understood using the eikonal equation.

We have shown that once the front velocity is known, the full interface profile can be computed numerically using a parallel flow approximation. Moreover, using a heuristic

argument, it has been shown that the velocity and the extension of the front could be expressed as functions of one single variable: $\Lambda = D_{\text{lock}}/HV_{\chi}$, where D_{lock} is the spreading diffusion coefficient computed for a lock-exchange gravity current *in the absence* of chemical reaction. The so-obtained constitutive laws, established for our experimental and numerical data, have been shown to also apply to other geometries found in the literature, such as the 2D gap between two parallel boundaries separated by a height H or cylindrical tubes, provided that the geometry-dependent coefficient D_{lock} is used in the variable Λ. Moreover, our model predictions correctly account for recent measurements with another autocatalytic reaction (chlorite-tetrathionate).

ACKNOWLEDGMENTS

It is a pleasure to thank Patrick De Kepper for giving us the PVA recipe. This work was partly supported by CNES (No. 793/CNES/00/8368), ESA (No. AO-99-083), Réseaux de Thématiques de Recherches Avancées "Triangle de la physique," and the Initial Training Network (ITN) "Multiflow." One of us (I.B.M.) was supported by a postdoctoral grant from the CNRS, whereas N.J. was supported by a grant from the French Ministry of Research (MESRT). All these sources of support are gratefully acknowledged.

[1] N. Jarrige, I. Bou Malham, J. Martin, N. Rakotomalala, D. Salin, and L. Talon, Phys. Rev. E **81**, 066311 (2010).
[2] L. Rongy, N. Goyal, E. Meiburg, and A. De Wit, J. Chem. Phys. **127**, 114710 (2007).
[3] J. A. Pojman, I. R. Epstein, T. J. McManus, and K. Showalter, J. Phys. Chem. **95**, 1299 (1991).
[4] G. Schuszter, T. Toth, D. Horvath, and A. Toth, Phys. Rev. E **79**, 016216 (2009).
[5] H. H. Huppert and A. W. Woods, J. Fluid Mech. **292**, 55 (1995).
[6] J. O. Shin, S. B. Dalziel, and P. F. Linden, J. Fluid Mech. **521**, 1 (2004).
[7] T. Séon, J. Znaien, D. Salin, J. P. Hulin, E. J. Hinch, and B. Perrin, Phys. Fluids **19**, 123603 (2007).
[8] S. M. Taghavi, T. Seon, D. M. Martinez, and I. A. Frigaard, J. Fluid Mech. **639**, 1 (2009).
[9] J. Martin, N. Rakotomalala, L. Talon, and D. Salin, "Viscous lock-exchange in rectangular channels" J. Fluid Mech. (in press), arXiv:1011.6262v1.
[10] R. Fisher, Ann. Eugen. **7**, 355 (1937).
[11] A. Kolmogroff, I. Petrovsky, and N. Piscounoff, Bull. de l'Univ. d'État à Moscou **1**, 1 (1937).
[12] S. K. Scott, *Oscillations, Waves, and Chaos in Chemical Kinetics, Physical*, Vol. 40 (Oxford University Press, New York, 2004).
[13] A. Hanna, A. Saul, and K. Showalter, J. Am. Chem. Soc. **104**, 3838 (1982).
[14] M. Böckmann and S. C. Müller, Phys. Rev. Lett. **85**, 2506 (2000).
[15] B. F. Edwards, Phys. Rev. Lett. **89**, 104501 (2002).
[16] M. Leconte, J. Martin, N. Rakotomalala, and D. Salin, J. Chem. Phys. **120**, 7314 (2004).
[17] J. Martin, N. Rakotomalala, D. Salin, and M. Böckmann, Phys. Rev. E **65**, 051605 (2002).
[18] E. Hinch, cited in Ref. 26 (2007).
[19] T. Yoshinaga, M. Tsuschida, Y. Toyose, H. Hiratsuka, and M. Yamaye, Anal. Sci. **20**, 549 (2004).
[20] D. Horváth and Á. Tóth, J. Chem. Phys. **108**, 1447 (1998).
[21] R. J. Field and M. Burger, *Oscillations and Traveling Waves in Chemical Systems* (Wiley, New York, 1985).
[22] J. Martin, N. Rakotomalala, L. Talon, and D. Salin, Phys. Rev. E **80**, 055101 (2009).
[23] A. Einstein, Ann. d. Phys. **17**, 549 (1905).
[24] D. Vasquez, J. Littley, J. Wilder, and B. Edwards, Phys. Rev. E **50**, 280 (1994).
[25] A. Toth, D. Horvath, and A. Siska, J. Chem. Soc. **93**, 73 (1997).
[26] Y. Hallez and J. Magnaudet, J. Fluid Mech. **630**, 71 (2009).